J Neurophysiol 123: 896–911, 2020.
First published January 22, 2020; doi:10.1152/jn.00614.2019.

RESEARCH ARTICLE | *Control of Movement*

Single-unit activity in marmoset posterior parietal cortex in a gap saccade task

Liya Ma,[1] Janahan Selvanayagam,[2] Maryam Ghahremani,[2] Lauren K. Hayrynen,[1] Kevin D. Johnston,[3] and Stefan Everling[1,2,3,4]

[1]*Robarts Research Institute, University of Western Ontario, London, Ontario, Canada;* [2]*Graduate Program in Neuroscience, University of Western Ontario, London, Ontario, Canada;* [3]*Departments of Physiology and Pharmacology, University of Western Ontario, London, Ontario, Canada; and* [4]*Brain and Mind Institute, University of Western Ontario, London, Ontario, Canada*

Submitted 27 September 2019; accepted in final form 15 January 2020

Ma L, Selvanayagam J, Ghahremani M, Hayrynen LK, Johnston KD, Everling S. Single-unit activity in marmoset posterior parietal cortex in a gap saccade task. *J Neurophysiol* 123: 896–911, 2020. First published January 22, 2020; doi:10.1152/jn.00614.2019.—Abnormal saccadic eye movements can serve as biomarkers for patients with several neuropsychiatric disorders. The common marmoset (*Callithrix jacchus*) is becoming increasingly popular as a nonhuman primate model to investigate the cortical mechanisms of saccadic control. Recently, our group demonstrated that microstimulation in the posterior parietal cortex (PPC) of marmosets elicits contralateral saccades. Here we recorded single-unit activity in the PPC of the same two marmosets using chronic microelectrode arrays while the monkeys performed a saccadic task with gap trials (target onset lagged fixation point offset by 200 ms) interleaved with step trials (fixation point disappeared when the peripheral target appeared). Both marmosets showed a gap effect, shorter saccadic reaction times (SRTs) in gap vs. step trials. On average, stronger gap-period responses across the entire neuronal population preceded shorter SRTs on trials with contralateral targets although this correlation was stronger among the 15% "gap neurons," which responded significantly during the gap. We also found 39% "target neurons" with significant saccadic target-related responses, which were stronger in gap trials and correlated with the SRTs better than the remaining neurons. Compared with saccades with relatively long SRTs, short-SRT saccades were preceded by both stronger gap-related and target-related responses in all PPC neurons, regardless of whether such response reached significance. Our findings suggest that the PPC in the marmoset contains an area that is involved in the modulation of saccadic preparation.

NEW & NOTEWORTHY As a primate model in systems neuroscience, the marmoset is a great complement to the macaque monkey because of its unique advantages. To identify oculomotor networks in the marmoset, we recorded from the marmoset posterior parietal cortex during a saccadic task and found single-unit activities consistent with a role in saccadic modulation. This finding supports the marmoset as a valuable model for studying oculomotor control.

common marmoset; posterior parietal cortex; single-unit recording; electrophysiology; Utah array; visually-guided saccade; gap effect

INTRODUCTION

Saccades are ballistic, conjugate eye movements that sample the visual environment and thereby serve as a gateway to higher cognitive functions. Distinct deficits in saccadic tasks can serve as both diagnostics for various neuropsychiatric disorders and indicators for underlying changes in the oculomotor network (Gooding and Basso 2008; Hutton and Ettinger 2006; Klein et al. 2000; Munoz and Everling 2004). Whereas the brainstem and superior colliculus (SC) control the generation of saccades (Keller and Edelman 1994; Waitzman et al. 1991), attention and other cognitive processes strongly modulate the reaction times of these movements (Hutton 2008). Although known to be mediated by cortical areas, including the frontal eye fields (FEF) and posterior parietal cortex (PPC) (Brown et al. 2004; DeSouza et al. 2003; Gaymard et al. 1998), the detailed microcircuits and computations involved in these processes are still not fully understood.

The common marmoset is a primate model that shares homologous functional networks with humans and macaque monkeys (Ghahremani et al. 2017), the most common nonhuman primate model. Behaviorally, the marmoset holds enormous potential for the study of primate communication and social behaviors (Miller et al. 2016). Given that eye movements are a crucial gauge for cognitive processes in primate studies, understanding the cortical mechanisms of oculomotor control is fundamental to cognitive studies in marmosets. Recent studies have demonstrated that marmosets can be trained to perform oculomotor tasks (Johnston et al. 2018) and display visual behaviors comparable to the macaques (Mitchell et al. 2014, 2015). Anatomically, the marmoset has a smooth cerebral cortex (lissencephaly), which permits perpendicular penetration of cortical layers and laminar analyses of local microcircuits in areas that are hidden in sulci in the macaque monkey, such as the FEF, the lateral intraparietal (LIP), middle temporal (MT), and medial superior temporal (MST) areas. Their lissencephaly also allows for functional mapping in each area with a chronically implanted planar electrode array (e.g., Utah array) (Ghahremani et al. 2019; Zavitz et al. 2016) and for the simultaneous monitoring of interacting areas using multiple arrays or electrocorticography grids.

Address for reprint requests and other correspondence: L. Ma, Robarts Research Inst., Univ. of Western Ontario, London, Ontario, N6A 5B7, Canada (e-mail: liyamariama@gmail.com).

The dorsal division of the marmoset PPC has been suggested to contain a putative homolog of the macaque LIP attributable to their similar pattern of myelination and the presence of large layer V pyramidal neurons (Rosa et al. 2009). Resting-state functional MRI studies corroborated this suggestion by identifying the same area as having triangulated connectivity with putative FEF and SC (Ghahremani et al. 2017). Recently, our group demonstrated that microstimulation of marmoset PPC evoked eye blinks and saccades (Ghahremani et al. 2019), as would be expected from an area homologous to area LIP in the macaque (Kurylo and Skavenski 1991; Shibutani et al. 1984; Thier and Andersen 1996, 1998). Here we report results from single-unit recordings using chronically implanted microelectrode arrays as a first characterization of the involvement of the marmoset PPC neurons in a simple saccade task. Upon completion of all recordings, we were able to evoke saccades and eye blinks with low-threshold microstimulation through the same arrays (Ghahremani et al. 2019), supporting a role of the area in modulating eye movements.

In both humans and macaques, a brief "gap" (typically 200 ms) intervening between the offset of the fixation point and the onset of the peripheral target is known to shorten subsequent saccadic reaction times (SRTs) (Saslow 1967) and elicit saccades with very short latencies, so-called express saccades (Fischer and Boch 1983). In macaque monkeys, increased activity in the gap period and higher pretarget activity levels for express compared with regular saccades were found in individual neurons in the SC (Dorris et al. 1997; Everling et al. 1999), the FEF (Dias and Bruce 1994; Everling and Munoz 2000), as well as in area LIP (Chen et al. 2013, 2016). In humans, EEG signals from the occipital-parietal network became enhanced before express saccades (Everling et al. 1996). The reduction in SRTs afforded by the gap has been attributed to both fixation release (Dorris and Munoz 1995; Fendrich et al. 1991; Reuter-Lorenz et al. 1991; Sommer 1994) and advanced preparation of saccadic motor programs (Paré and Munoz 1996). In comparison, the generation of express saccades can be explained by motor preparation alone as demonstrated in the SC (Dorris et al. 1997; Everling et al. 1998), the FEF (Everling and Munoz 2000), and area LIP in macaque monkeys (Chen et al. 2013, 2016). Given the anatomical and functional connectivity between marmoset PPC, FEF, and SC (Collins et al. 2005; Ghahremani et al. 2017; Majka et al. 2016; Reser et al. 2013), we hypothesize that it plays a role in the motor preparation preceding the gap effect and express-like saccades.

Here we report results from microelectrode array recordings from the PPC of marmoset monkeys while they performed visually guided saccades with or without a 200-ms gap period (Gap vs. Step trials) in a randomly interleaved fashion. As we showed previously (Johnston et al. 2018), marmosets displayed shorter SRTs in the gap than step trials. Our findings suggest that the marmoset PPC plays a role in modulating saccadic motor preparation, which contributes to the gap effect and the generation of short-SRT saccades in the gap task.

MATERIALS AND METHODS

Animals

Two male common marmosets (*Callithrix jacchus*), weighing 440 g and 451 g at the age of 2.5 and 4 yr, respectively, were used in the study. All procedures performed were approved by the Animal Care Committee of the University of Western Ontario Council on Animal Care and in accordance with the Canadian Council of Animal Care policy on laboratory animal use.

After the initial acclimatization to the custom-designed chair restraint, over the course of several weeks, the marmosets were gradually trained to sit quietly facing the monitor and to consistently lick the sipper tube for their preferred liquid reward, which was delivered intermittently (Johnston et al. 2018). For *marmoset B*, the preferred reward was sweetened condensed milk mixed with water in a 2:1 ratio, and for *marmoset W* this was corn syrup mixed with water in a 1:1 ratio. Once they could sit calmly for 45 minutes, the first surgery was performed to install a head restraint/recording chamber (Johnston et al. 2018). A second surgery, for implantation of the microelectrode array, took place after the monkeys became proficient with the behavioral task.

Surgical Procedures

For both surgeries, the animals were anesthetized with ketamine and maintained with intravenous propofol and gaseous isoflurane (Johnston et al. 2018). Their heart rate, SpO_2, temperature, and breathing were continuously monitored by an experienced veterinary technician. After each surgery, the marmosets received postsurgical treatments, including analgesics and antibiotics, to minimize pain or discomfort, under the oversight of a university veterinarian.

In the first surgery, a custom-designed combination head restraint/recording chamber (Johnston et al. 2018) was attached to the skull with UV-cured dental adhesive and resin [All-Bond Universal and Duo-Link, Bisco Dental Products (Canada), Richmond, BC, Canada]. Together with a custom-designed protective cap, the chamber would serve to protect the electrode array after its implantation. After the animals were well trained on the task, they underwent a second surgery, in which a parietal craniotomy was made inside the recording chamber at 1.4 mm anterior and 6 mm lateral to the interaural midpoint, and a 32-channel Utah array (Blackrock Microsystems, Salt Lake City, UT) was implanted. The positioning of the array was guided by both stereotaxic coordinates of area LIP (Paxinos et al. 2012) and the location of a posterior parietal area functionally connected to the SC (Ghahremani et al. 2017). Additionally, we were guided by the location of a small blood vessel that corresponded to the location of the shallow intraparietal "dimple" and resembled the positioning of a blood vessel in the macaque intraparietal sulcus. Before insertion of the array, we secured a ground screw in a small burr hole made posterior to the craniotomy. Arrays were manually inserted so that they straddled the intraparietal dimple and covered as much of the dimple as possible along the anterior-posterior axis. The connecting wires and the connector were secured inside the chamber using dental resin. The grounding wires were then tightly wound around the ground screw to ensure electrical connection before being secured with dental resin. The array and craniotomy were protected by a very fine layer of gel foam and medical-grade silicone elastomer adhesive (Kwik-Sil; World Precision Instruments, Sarasota, FL) before being covered by dental resin.

Behavioral Training and Paradigm

On the day before each training or recording session, the animals received mild food restriction; the size of their second of two daily meals was reduced to 80% of their ad libitum consumption amount. On the training/recording day, the session always took place before the first of their two daily meals (Johnston et al. 2018). During training, the animals received their preferred liquid reward upon the successful completion of each trial.

Training on the goal-directed saccade task consisted of two steps, fixation training and saccade training. During fixation training, the animals learned to start fixating within 4 s and maintain the gaze for

500 ms on a marmoset face 0.8° × 0.8° in size within a 5° × 5° electronic window. The required duration of fixation gradually increased from 20 to 500 ms. The possible location for this stimulus was gradually increased from 1 (center only) to 3 (center, left, and right) and was used in a random order. Trials on which the animal failed to acquire or maintain fixation were followed by a 5,000-ms time-out period. Once the animal was able to respond to the stimulus in each location as required, the electronic window was reduced to 3° × 3°. During saccade training, if the fixation was maintained successfully for 500 ms, the central stimulus was replaced immediately by a second target presented at 5° to the left of fixation. The animals were rewarded if they initiated a saccade to the target within 1,000 ms and maintained fixation for 10 ms within a 5° × 5° window surrounding the target. Once the animal acquired this response, a second possible target 5° to the right of fixation was used, first on alternating 10-trial blocks with the left target, then on randomly selected trials. When the animals became proficient at the task, we reduced the time allowed between fixation stimulus offset and saccade onset to 500 ms, the same criterion commonly used for macaque monkeys, and replaced each face stimulus with a white dot (0.25° in diameter, luminance 10 cd/m^2) at the center of the 5° × 5° window. The same fixation dot was then used in the goal-directed saccade paradigm. The same dark background (2 cd/m^2) was used in both training and the goal-directed saccade task.

The goal-directed saccade paradigm included Step and Gap conditions (Fig. 1*A*). Each trial began with the appearance of a white dot (see above for details) at the center of the screen. The animals were required to initiate fixation within 3 s and maintain the gaze within a window of 1.5° × 1.5° for 700-900 ms. On Step trials, concurrent with the offset of the fixation spot, a peripheral target was presented randomly to the left or right by 5°. The target is a white dot greater in size (0.8° in diameter) and equal in luminance to the fixation dot (10 cd/m^2). The animals were rewarded if they generated a saccade within 500 ms and if the saccade endpoint fell within a 3° × 3° window surrounding the target. This criterion for valid visually guided saccades is the same as that traditionally used for macaque monkeys (e.g., Everling et al. 1998). On Gap trials, after 500–700 ms of fixation, the spot was extinguished for a "gap period" of 200 ms, during which the

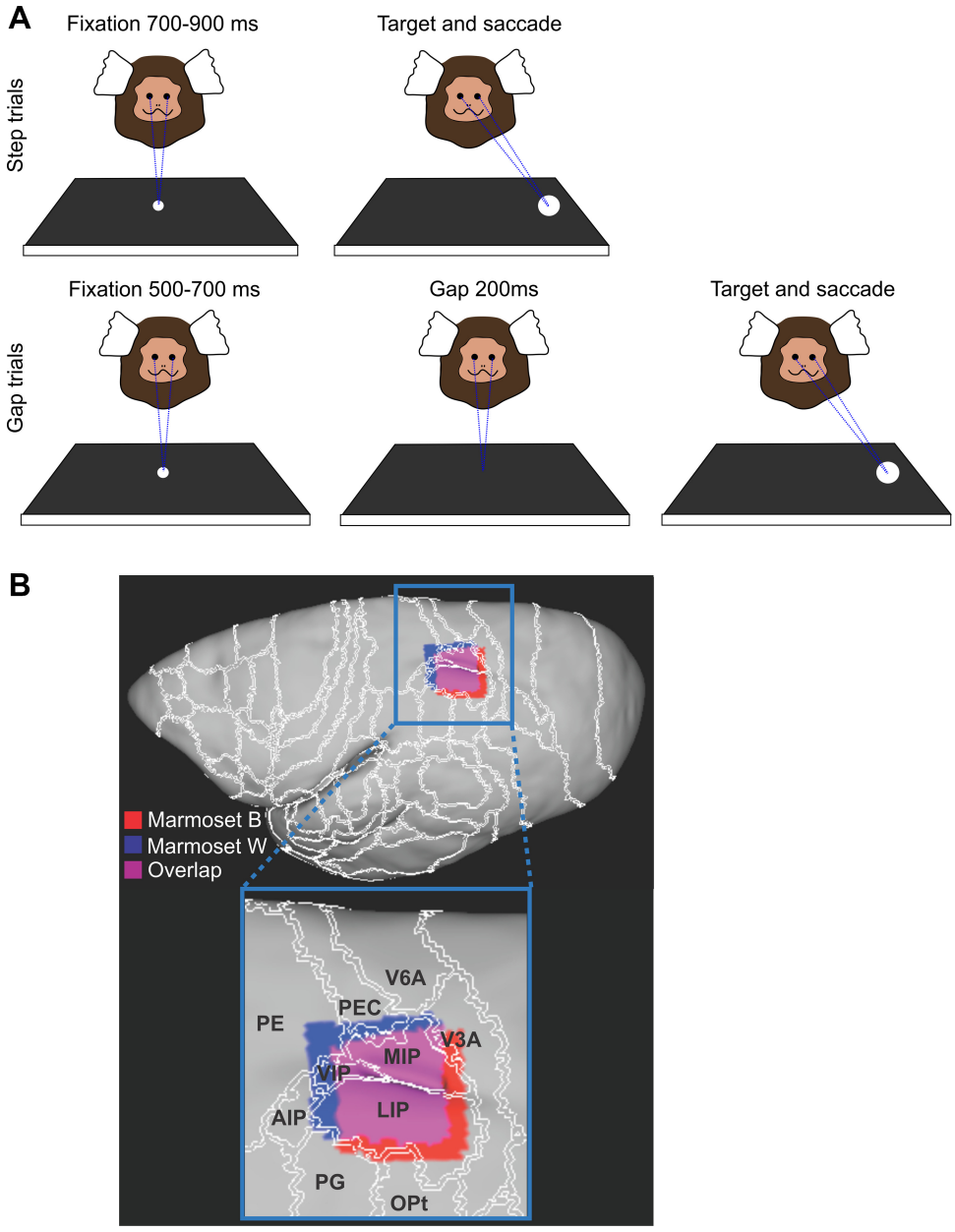

Fig. 1. Schematic illustration of the goal-directed saccade paradigm and positioning of the microelectrode arrays. *A*: 2 trial types and the left/right location of the saccadic target were randomly interleaved. In Step trials, the animals had to maintain fixation on the central white dot for a random interval between 700 and 900 ms before its offset and the onset of the peripheral target, to which they had to make a saccade (*top*). In Gap trials, the fixation dot extinguished after an interval between 500 and 700 ms, and the target came on after a 200-ms gap period, during which fixation had to be maintained despite of the lack of any visual display (*bottom*). A liquid reward was delivered if the animal made a saccade to the target within 500 ms. *B*: array positioning based on ex vivo MRI and in vivo micro-CT scan for the 2 marmosets, respectively. *Top*: array locations for *marmoset B* (red) and *marmoset W* (blue) registered on the surface space of the left hemisphere of the brain, with their overlap shown in purple and cortical boundaries overlaid in white. *Bottom*: zoomed-in view of the recorded area with neighboring areas labeled according to the NIH digital 3D atlas of the marmoset brain (Liu et al. 2018). LIP, lateral intraparietal area; MIP, medial intraparietal area; VIP, ventral intraparietal area; AIP, anterior intraparietal area; OPt, occipito-parietal transition area; V6A, visual area 6A; V3A, visual area 3A.

animals were required to maintain their gaze within the same electronic window. The onset of a peripheral target marked the end of the gap period. The animals were rewarded if they generated responses that met the same criteria as in the Step condition. Gap and Step trials were randomly interleaved. The animals' eye positions were recorded and digitized at 1,000 Hz using an Eyelink 1000 infrared pupillary tracking system (SR Research, Mississauga, ON, Canada).

Gaze Stability

To quantify gaze stability and its change, we calculated the total amount of gaze shift in each Fixation and Peristimulus period. This was obtained by summing the magnitude of gaze shift in each 1-ms bin, defined as the amplitude of the vector sum of both horizontal and vertical eye movement with reference to the previous 1-ms bin. We then compared the total gaze shift from the Fixation to the Peristimulus period in each trial type to see whether the gap affected gaze stability. We also examined whether changes in neuronal activity across trials were correlated with the magnitude of gaze shift, which could potentially confound any gap-related effect in single-unit activity.

Recording and Data Analysis

Neural activities, including local field potentials and spike trains, as well as eye-tracking data were recorded using a multiacquisition processor system (Plexon, Dallas, TX) for *marmoset B* and the Open Ephys acquisition board (https://www.open-ephys.org/) and digital headstages (INTAN, Los Angeles, CA) in *marmoset W*. Data collected with both systems were converted to Neuroexplorer (nex) files, and single units were isolated by applying principal component analysis (PCA) in 2D and 3D with the Plexon Offline sorter (Plexon, Dallas, TX). Other features, such as auto- and cross-correlogram and temporal stability in the waveforms, were also consulted to avoid further division of the activity of one unit. Low-amplitude waveforms without a distinct shape were considered multiunit activity and were excluded from further analysis. Spiking activities of well-isolated units were then analyzed in MATLAB (MathWorks, Natick, MA; RRID:SCR_001622). Single units with firing rates <0.3 Hz were excluded from further analyses.

Because of the use of chronic, nonadjustable arrays, it was difficult to ascertain whether the same units were sampled again in a subsequent session. High correlation in waveforms may suggest that a unit is detected again (Nicolelis et al. 2003), yet different units of the same neuronal subtype often share similar waveforms. High correlation in interspike interval histograms (ISIH) has also been used effectively to quantify repeated detection of the same units (Dickey et al. 2009). However, the reliability of this method depends on the stability of the ISIH, which is in turn affected by changes in the level of arousal and attention (Harris and Thiele 2011; Reimer et al. 2014; Vinck et al. 2015). Thus the probability of repeated sampling could not be established for the Utah arrays using the present task design, and we decided to treat units recorded on different sessions as independent. This is a limitation in the use of chronic, nonadjustable arrays in a task without full control over the animals' level of arousal and attention.

For behavioral analysis, we included only correctly performed trials with SRTs <350 ms. We also excluded anticipatory saccades with an SRT <48 ms and 77 ms, respectively, for *marmosets B* and *W*, as these saccades had only a 50% probability of being correct.

For the analyses of neuronal activities, we focused on three behavioral epochs, the Fixation period, the Peristimulus period, and the Visuomotor period. The Fixation period was defined as the interval from 400 ms to 201 ms before the onset of the peripheral target. In Gap but not Step trials, the end of the Fixation period coincided with the offset of the fixation point, or the onset of the gap period. The Peristimulus period was defined as the interval from 165 ms before to 34 ms after the onset of the peripheral target. In Gap trials, this period nearly coincided with the gap period, starting 35 ms after the offset of the fixation dot (Fig. 1*A*). The first 34 ms after target onset still belonged to the gap period because that single-unit target-related response started no sooner than 35 ms after target onset (Fig. 5*C*). This may suggest that the visual signal takes at least 35 ms to reach the PPC in the marmosets. The Visuomotor period was defined as the interval from 35 ms to 134 ms after target onset, 100 ms in duration. Given that it ended later than the reaction times of many saccades, activities captured in this window could also reflect postsaccade processes.

Parametric statistical tests, such as *t*-tests and ANOVAs, were used provided that each group involved in the test had a sample size >30. For the correlation analysis (Fig. 7), we used the nonparametric Spearman's rho because the parametric Pearson's rho assumes strict normality in each group of data tested. To determine whether the correlation coefficients were significantly different from zero at the group level, we used one-sample *t*-tests with adjustments for family-wise false discovery rate (Benjamini and Hochberg 1995; Groppe et al. 2011).

Spike Density Function

To evaluate the relationship between neural activity, target onset, and saccade onset, continuous spike density functions were constructed. The activation waveform was obtained by convolving each spike with an asymmetric function that resembled a postsynaptic potential (Hanes and Schall 1996; Thompson et al. 1996). The advantage of this function over a standard Gaussian function (Richmond and Optican 1987) is that it accounts for the fact that spikes exert an effect forward but not backward in time. We used this convolution method in all line plots of single-neuron or group-averaged activity but not on data used in any statistical tests or shown in bar graphs.

Principal Component Analysis

To find the onset of gap-related response in gap neurons, we conducted a PCA using the *pca* function in MATLAB. Each 10-ms time bin during the last 400 ms before stimulus onset was treated as one variable (a total of 40), and the trial-averaged activity of each gap neuron during the same period contributed one observation (a total of 54). Two separate PCAs were done for Gap and Step trials, respectively. PC1 from both analyses is shown in Fig. 3*B*, representing the most dominant temporal pattern across all gap neurons. The total variance accounted for by all PCs was computed by dividing the cumulative sum by the sum of eigenvalues of the covariance matrix of the input data.

Confirming Array Location

Ex vivo MRI was conducted to confirm the positioning of the array for *marmoset B*. As *marmoset W* is involved in additional experiments, in vivo micro-CT scan was used as an alternative method to confirm the array location.

Ex vivo MRI scan. To prepare for the MRI, *marmoset B* was euthanized through transcardial perfusion, and its brain was extracted at the end of the procedure. Anesthesia was induced with 20 mg/kg of ketamine plus 0.025 mg/kg medetomidine and maintained with 5% isoflurane in 1.4-2% oxygen at a state deeper than the surgical plane, with no response to cornea touching or toe pinching. The animal was then transcardially perfused with 200 ml of phosphate-buffered saline, followed by 200 ml of 10% formaldehyde-buffered solution (formalin). The brain was then extracted and stored in 10% buffered formalin for over a week. On the day of the scan, the brain was transferred and immersed in a fluorine-based lubricant (Christo-lube; Lubrication Technology) to improve homogeneity and avoid susceptibility artifacts at the boundaries. The ex vivo image was then acquired using a

9.4T, 31-cm horizontal bore magnet (Varian/Agilent) and Bruker BioSpec Avance III console with the software package Paravision-6 (Bruker BioSpin) and a custom-built 15-cm-diameter gradient coil with 400 mT/m maximum gradient strength (xMR, London, Ontario, Canada). An ex vivo T2-weighted image was acquired with the following scanning parameters: repetition time (TR) = 5 s, echo time (TE) = 45 ms, field of view (FOV) = 40 × 32, image size = 160 × 128, slice thickness = 0.5 mm.

To identify the location of the array, the resulting T2-weighted image was registered to the NIH marmoset brain atlas (Liu et al. 2018) using the registration packages of the FSL software (fMRI Software Library: https://www.fmrib.ox.ac.uk/). Upon visual examination of the image, an indentation of comparable size to the array (2.4 × 2.4 mm) was identified on the surface of the cortex within the PPC that represented the array location. The location of this region of interest was interpolated on the cortical surface to create a mask across this indentation, meant to represent an approximation of the array location. The mask was then projected onto the surface space in CARET toolbox (Van Essen et al. 2001) using a surface-based version of the NIH volume template that was kindly provided by the authors of the NIH marmoset brain template (Liu et al. 2018). The array mask was then compared to the area LIP as defined by the parcellated regions of the NIH template, which was also projected on CARET surface space.

In vivo micro-CT scan. Marmoset W was imaged in a live-animal micro-CT scanner (eXplore Locus Ultra; GR Healthcare Biosciences, London, ON) to identify the array location. Before the scan, the animal was anesthetized with 15 mg/kg ketamine mixed with 0.025 mg/kg medetomidine. He was then placed on his back on the CT bed with arms positioned down along his sides and inserted into the scanner. X-ray tube potential of 120 kV and tube current of 20 mA were used for the scan, with the data acquired at 0.5° angular increments over 360°, resulting in 1,000 views. The resulting CT images were then reconstructed into 3D with isotropic voxel size of 0.154 mm. Heart rate and SpO_2 were monitored throughout the session. At the end of the scan, the injectable anesthetic was reversed with an IM injection of 0.025 mg/kg Ceptor.

The location of the array was clearly identified within marmoset PPC by visual inspection of the CT image. To find the location of the array with respect to the NIH template, the acquired CT image was brain extracted while including the trace of the array across the boundary of the cortex. The brain-extracted image was then registered to the NIH marmoset brain atlas (Liu et al. 2018) using the FSL software (fMRI Software Library: https://www.fmrib.ox.ac.uk/). Similar to the ex vivo MRI data, an ROI mask was created over the traces of the array across the surface of the cortex to represent the location of the array. This mask along with the actual location of area LIP was projected on the surface space using CARET to compare the positioning of the array to area LIP.

RESULTS

We recorded neural activity through 32-channel Utah arrays in 13 sessions in *marmoset B* and 14 sessions in *marmoset W* while the monkeys performed randomly interleaved Gap and Step trials (Fig. 1*A*). The recording locations in the PPC, identified using either in vivo micro-CT scan or ex vivo MRI combined with the NIH marmoset brain atlas (Liu et al. 2018), are shown in Fig. 1*B*.

Behavior

In total, *marmoset B* performed 2,662 correct trials, and *marmoset W* performed 2,729 correct trials. The sessions had a mean duration of 32.6 min (SD = 8.2 min). Trials in which the animal made saccades that were anticipatory, incorrect, or with SRTs >350 ms were excluded from further analyses. Saccades with an SRT <48 ms and 77 ms, respectively, for *marmosets B* and *W* had only a 50% probability of being correct and were excluded as anticipatory saccades.

On the basis of the trial selection criteria, we plotted the distributions of SRTs in Gap and Step trials, respectively (Fig. 2, *A* and *B*). The solid bars indicate the percentage of correct trials in each SRT bin, the shaded bars denote the percentage of error trials, and the open bars show the percentage of anticipatory saccades. We also separated the SRTs by saccadic direction, ipsilateral saccades toward saccadic targets on the

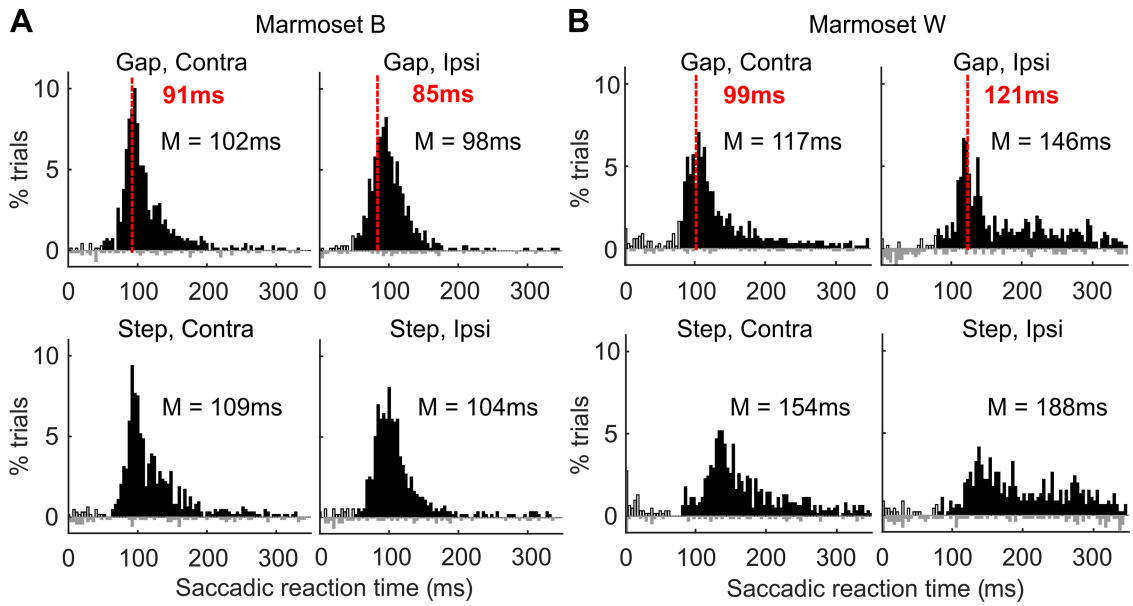

Fig. 2. Saccadic reaction time (SRT) histograms showing the percentage of trials of each type (e.g., Gap trials with contralateral saccades) with SRTs in 4-ms bins between 0 and 350 ms. Solid bars, correct trials; shaded bars, error trials; open bars, anticipatory saccades. Red dashed line, boundary of the shortest quartile of SRTs. Correct saccades with SRTs shown to the left of the line were classified as "short-SRT saccades," and those to the right were "long-SRT saccades." The median (M) of SRTs was also shown for each trial type and direction. *A*: SRT histograms of saccades performed by *marmoset B*. *B*: SRT histograms of saccades performed by *marmoset W*. Contra, contralateral saccades; Ipsi, ipsilateral saccades.

same side as the electrode arrays (Fig. 2, *A* and *B*, *bottom*) and contralateral saccades toward the opposite side (Fig. 2, *A* and *B*, *top*). All these distributions were significantly nonnormal in both animals (Kolmogorov-Smirnov tests, KS stats ≥ 0.5, $P \leq 5.0 \times 10^{-20}$); thus nonparametric tests were used to compare SRTs across tasks. In both marmosets, the SRTs of correct trials were significantly shorter during Gap than Step trials (rank sum test, *marmoset B*: $Z = -6.32$, $P = 2.6 \times 10^{-10}$, *marmoset W*: $Z = -13.4$, $P = 3.9 \times 10^{-41}$). Unlike macaque monkeys, but not unlike humans, the SRTs in Gap trials were not distinctively bimodally distributed. Hence, we could not objectively separate the responses into express and regular saccades. Instead, we separated the trials into those with short-SRT and long-SRT saccades (Fig. 2, *A* and *B*), based on whether their SRTs fell into the shortest quartile (to the left of red dashed lines) or not (to the right of the red dashed lines).

Response of Single Units to the Gap

A total of 361 well-isolated single units were recorded from both marmosets (*marmoset B*: $n = 173$, *marmoset W*: $n = 188$). Without a reliable method for establishing whether the same unit was sampled across sessions (see *Recording and Data Analysis* in MATERIALS AND METHODS), we decided to count single units from each session toward the population. This is a limitation of the use of chronic, nonadjustable array in a task where the animals' level of attention and/or arousal may fluctuate. We found that 15% were sensitive to the gap period. To identify these neurons, we followed the method used in previous studies in macaque monkeys (Ben Hamed and Duhamel 2002; Tinsley and Everling 2002) and performed for each unit a paired *t*-test between activity during the Peristimulus and Fixation periods in Gap trials. The Peristimulus period lasted from 165 ms before target onset to 34 ms after target onset, which in Gap trials was the same as the 200-ms period starting from 35 ms after the offset of the fixation point. For the Fixation period, we chose the 200 ms before the offset of the fixation dot, or 400 ms to 201 ms before target onset. We found 54 neurons that responded significantly to the gap ($P < 0.05$), constituting 15% of the total population and were referred to as the "gap neurons."

Because these neurons were detected using their Gap-trial activities only, we then examined their Peristimulus response, defined as the change in firing rates from the Fixation to the Peristimulus period, across trial types. We found that the Peristimulus response of gap neurons was smaller in magnitude in Step than in Gap trials (paired *t*-test, $t_{53} = 6.30$, $P = 6.1 \times 10^{-8}$), which was not the case for the other neurons (paired *t*-test, $t_{218} = 0.71$, $P = 0.48$). We plotted the absolute value of the Peristimulus response in Gap trials against those in Step trials, respectively, for gap neurons (red dots) and the other neurons (black circles). The vast majority (92.6%) of the red dots were above the dashed unity line, indicating a greater Peristimulus response in Gap trials.

To determine the precise timing of the gap-related response, we performed a PCA on 400 ms of prestimulus activity of the gap neurons (see MATERIALS AND METHODS). We treated the trial-averaged activity of each gap neuron as an observation ($n = 54$) and each 10-ms time bin as a variable ($n = 40$). In Gap trials, the most dominant temporal pattern in this period (Fig. 3*B*, *top*) contains a prominent deflection at 70 ms after the offset of the fixation dot (or 130 ms before stimulus onset; dashed line). In Step trials, the most dominant pattern is essentially flat throughout the last 200 ms of fixation (Fig. 3*B*, *bottom*). The top principal component (PC1) accounted for 78.8% and 89.5% of total variance in time in Gap-trial and Step-trial activities, respectively. This difference in temporal pattern is visible in the mean activity of gap neurons with a positive response ($n = 37$); Fig. 3*C* shows their Peristimulus activity, *z*-score standardized against Fixation-period activity. At 130 ms before stimulus onset (or 70 ms after fixation offset; dashed line), their activity in the two trial types started to diverge as the gap was associated with steeper rise in firing rates (red and magenta curves, Fig. 3*C*).

Unexpected from the selection criterion for the gap neurons was the effect of the peripheral target, reflected as sharp increases in averaged activity starting 35 ms after target onset, in trials with contralateral targets (red and dark blue) but not those with ipsilateral targets (magenta and light blue, Fig. 3*C*). That is, posterior parietal gap neurons in the left hemisphere responded to the target when it was presented in the right half of the visual field.

The activity of representative gap neurons is shown in Fig. 3, *D–G*. In the raster plots, each black dot represents a single action potential during a Gap trial, and a gray dot marks a single spike in a Step trial. Each row illustrates the activity of the neuron from 200 ms before to 300 ms after target onset in one trial. For each task, the trials were sorted by saccade onset as marked by red diamonds. The curves in Fig. 3, *D–G*, display the trial-averaged level of activity in each consecutive 10-ms bins, with the dashed lines depicting the standard error of the mean. Figure 3*D* shows a neuron with activity that ramped up in the second half of the peristimulus period in Gap (black curve) but not Step trials (gray curve). Figure 3*E* shows a different type of response among the gap neurons, a sharp rise in activity several tens of milliseconds after the offset of the fixation point. Both neurons also displayed target-related activity ~70 ms after target onset in both Gap and Step trials. In addition to a positive gap response, the neuron shown in Fig. 3*F* also displayed saccade-related modulation, activity suppression at around saccade onset, followed by an increase in activity starting ~20 ms afterward. Figure 3*G* shows a gap neuron with a negative response after fixation offset, followed by a target-related response at around 35 ms after target onset. Notably, all three neurons in Fig. 3, *D*, *E* and *G*, displayed an abrupt change in activity at ~70 ms after fixation offset, which is consistent with the finding from PCA (Fig. 3*B*). We characterize target-related responses in the next section.

It remains possible that the significant change in neuronal activity from Fixation to Peristimulus period was related to a change in gaze stability especially in Gap trials. We therefore compared the amount of shift in gaze during the two periods, in both Gap and Step trials. We found significant changes in 7 out of the 27 sessions (26%), with an increase in gaze shift from Fixation to the Peristimulus period in 2 sessions and a decrease in 5 sessions in Gap trials. In Step trials, we found only 1 session (3.7%) with a significant increase in gaze shifts. Thus the gap may alter gaze stability, although this influence can come in both directions.

We then examined whether changes in neuronal activity were correlated with gaze shifts. Of 54 Gap neurons, we found only 3 (5.6%) that had a Peristimulus response that correlated

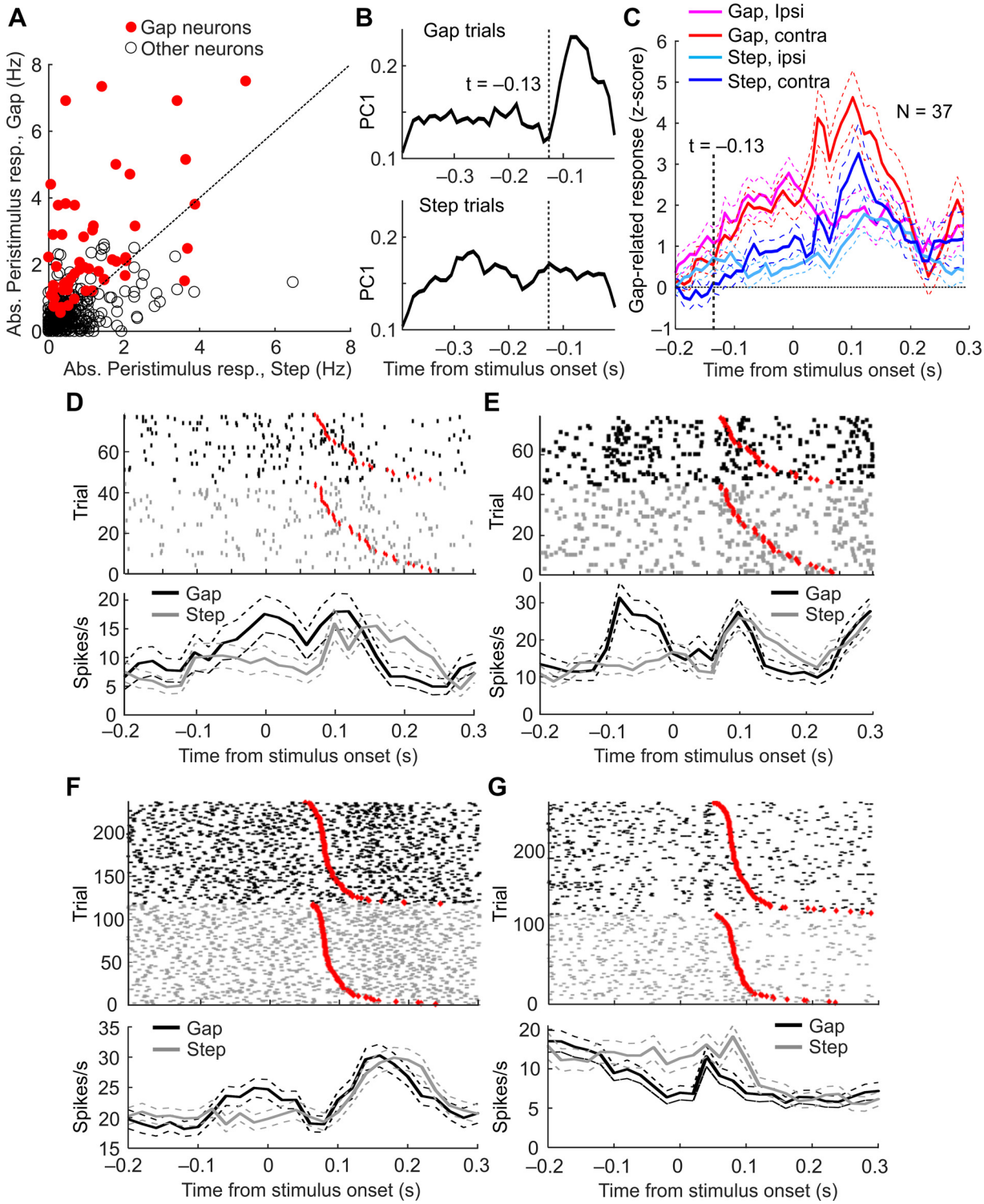

Fig. 3. Gap neurons and their peristimulus change in activity. *A*: absolute peristimulus response in Gap (ordinate) vs. Step (abscissa) trials, from gap neurons (red dots) and all the other neurons (black circles). *B*: most dominant temporal pattern in gap neuron activities in Gap (*top*) vs. Step (*bottom*) trials, as revealed by principal component analyses. The gap-related response was observed ~70 ms after fixation offset. PC1 refers to the principal component that accounted for the greatest amount of temporal variance in the neural activities. *C*: standardized peristimulus response averaged across all gap neurons with an excitatory response. These neurons also had a second response to the target, with a preference for contralateral targets emerging at 35 ms following their onset. *D*: example of a gap neuron that showed gradual increase in activity toward the end of the Peristimulus period in Gap but not Step trials. Each tick mark denotes a single action potential. Red diamonds mark saccadic onsets. *E*: example of a gap neuron that displayed a sudden increase in activity ~70 ms following the offset of the fixation dot. Both neurons in *D* and *E* also showed a target-related response starting ~60 ms following target onset. *F*: neuron with gap-related activity enhancement, as well as saccade-related modulation in activity. *G*: neuron with gap-related reduction in activity, followed by a target-related rise in firing rate.

with the magnitude of gaze shifts (Spearman's $r = 0.18$, -0.22, and -0.21, respectively; $P < 0.05$). None of the 3 neurons had this correlation with gaze shift in Step trials ($P \geq 0.27$, $r \leq 0.093$), and 2 of the 3 neurons did not have such correlation when both types of trials were combined. Thus the correlations were specific to Gap trials in 2 of the 3 neurons. The remaining neuron was recorded in a session with no Fixation-to-Peristimulus change in gaze stability in Gap trials; thus the correlation with gaze shift could not have affected its overall gap-related response. Thus the Peristimulus response of Gap neurons could not be explained by a change in gaze stability.

The 2D configuration of the Utah array allowed us to estimate the spatial distribution of the gap neurons along the anterior-posterior (x-axis, Fig. 4) and medial-lateral (y-axis) axes within the PPC. Given that the arrays straddled the intraparietal dimple, we asked whether gap neurons concentrated more in the lateral half of the arrays, which was more likely to be in the LIP according to the atlas, and found no evidence for this. Because neurons were not detected evenly across all sites, we plotted the percentage of gap neurons out of all recorded neurons at each site for each marmoset (Fig. 4). We found that gap neurons did not concentrate on either medial or lateral half of the array for *marmoset B* (Mann-Whitney U-test, $U = 292$, $P = 0.26$), and for *marmoset W* they were more likely to be detected by the medial half of the channels ($U = 326$, $P = 0.006$). We also compared the rate of gap neuron detection between the anterior and posterior halves of the arrays and found no difference in either animal (Mann-Whitney U-test, $U = 220.5$ and 250, $P = 0.078$ and 0.55, respectively).

Response of Single Units to the Saccade Target

In the macaque monkey, the PPC is known to contain neurons that are responsive to the visual target and those responsive to saccade preparation (Andersen et al. 1985; Ben Hamed et al. 2001; Colby et al. 1996). We therefore searched for PPC neurons in the marmosets that responded to the saccade target, or target neurons for short. Because we did not use a delayed response task, we defined the change in activity from the Fixation (400 ms to 201 ms before target onset) to the Visuomotor period (35 to 134 ms after target onset) as the Visuomotor response without any attempt to separate the visual and motor aspects of the signal. On the basis of a paired t-test between these periods, we identified 142 or 39.3% of all recorded neurons as being significantly responsive to the Visuomotor period in at least one type of trials (Fig. 5*A*, *left*). Notably, the activity of these neurons rose abruptly at 35 ms after target onset, suggesting the arrival of the visual signal at the PPC and supporting our definition of the boundary between the Peristimulus and Visuomotor periods. Among these neurons, 40.9% responded only in Gap trials, 24.7% responded only in Step trials, and the remaining 34.5% responded in both trial types. Together the normalized activity of these 142 target neurons was contrasted with the remaining 219 neurons (60.7%; Fig. 5*A*, *right*). We went on to compare the magnitude of the Visuomotor response of the neurons between trial types, as plotted in Fig. 5*B*. On average, the target neurons (red dots) showed a stronger Visuomotor response in Gap than Step trials (paired t-test, $t_{141} = 3.15$, $P = 0.002$), which was not the case among the other neurons (paired t-test, $t_{218} = -0.83$, $P = 0.41$; black circles, Fig. 5*B*). Thus, not only were there more neurons responsive to the target following a gap period, but this response was also stronger than in Step trials.

Because the gap and target neurons were identified independently, the two groups were not mutually exclusive. Indeed, 36 neurons belonged to both groups, constituting 10% of all recorded neurons, 25.4% of target neurons, and 66.7% of gap neurons. Given the existence of these "dual-response" neurons, we asked whether they were responsible for the task effect on the Visuomotor response. To answer this question, we split the target neurons into dual-response and non-gap target neurons and tested the Visuomotor response across all neurons using a mixed-model ANOVA with task as the within-subject factor and cell type (dual response, target only and other neurons) as the between-subject factor. We found a significant task × cell-type interaction ($F_{2,358} = 12.7$, $P = 4.9 \times 10^{-6}$). Although the two types of target neurons were similar in their Visuomotor response in Step trials (post hoc Tukey's test: $P = 0.41$), the dual-response neurons responded more strongly on Gap trials ($P = 0.0032$). In short, target neurons preferentially responded to contralateral targets across trial types; 10% of all PPC neurons, not only responded to the gap period, but also responded more strongly to targets following the gap, potentially contributing to the gap effect.

Four examples of target neurons are shown in Fig. 5, *C–F*, all of which displayed a sharp increase in activity at ~35 ms following the onset of the target. The cell shown in Fig. 5*C* is

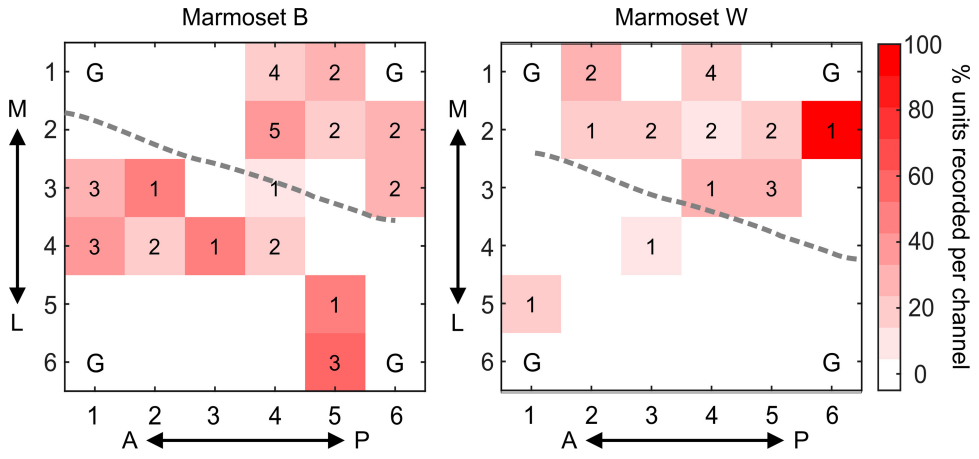

Fig. 4. Topographical distribution of gap neurons in both actual number and as a percentage of all neurons recorded from each channel (shown as different shades of red) in *marmosets B* (*left*) and *W* (*right*) in the marmoset posterior parietal cortex. In each panel, the abscissa corresponds to the anterior-posterior axis of the brain, whereas the ordinate corresponds to the medial (*top*)-lateral (*bottom*) axis. The gray dashed lines mark the location of the intraparietal dimple in each animal. M, medial; L, lateral; A, anterior; P, posterior; G, grounding channels.

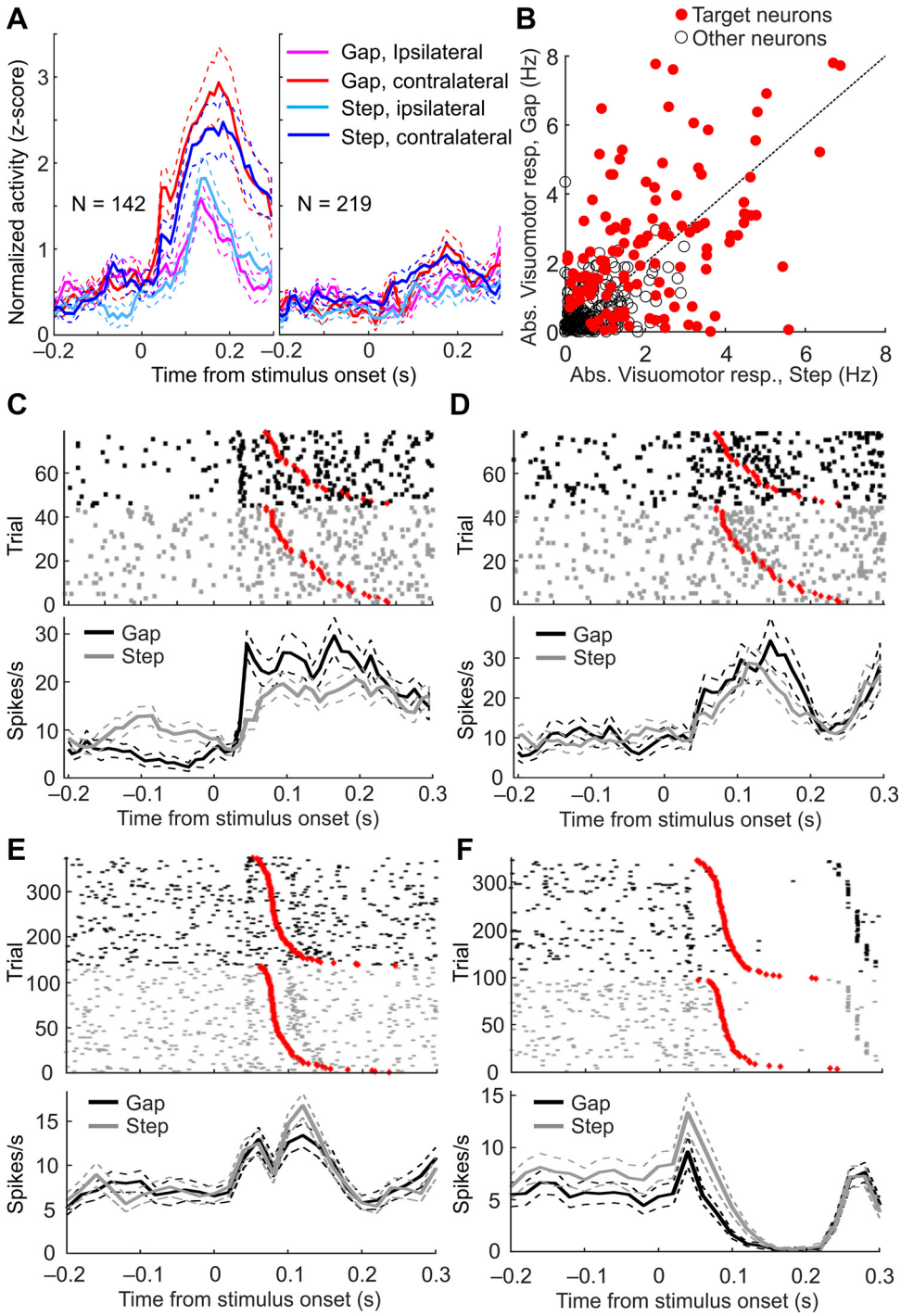

Fig. 5. Target neurons and their target-related change in activity. *A*: standardized activities averaged across all target neurons (*left*), compared with the response of nontarget neurons (*right*). In target neurons, the response starts at 35 ms after target onset, with a strong preference for contralateral targets. *B*: absolute Visuomotor response in Gap (ordinate) vs. Step (abscissa) trials, from target neurons (red dots) and all the other neurons (black circles). *C*: example of a target neuron with a steep rise in activity at ~35 ms following target onset. This response was more consistently timed in Gap than in Step trials. The same neuron also responded differently during the peristimulus period in Gap and Step trials. Each tick mark denotes a single action potential. Red diamonds mark saccadic onsets. *D*: example of a target neuron that displayed a sudden increase in activity ~35 ms following target onset. Unlike *C*, this neuron did not respond to the gap period. *E*: target neuron with a phasic response to the target at 35 ms, followed by another phasic response that appeared to be aligned with saccadic offset. *F*: target neuron with a phasic response to the target at 35 ms, followed by an ~200-ms period of complete silence.

also a dual-response cell, displaying an inhibitory response during the gap period and a stronger response to the saccadic target in Gap trials. Notably, this neuron also encoded a saccade-related signal, as indicated by its consistent reduction of activity after saccadic onset (marked by red diamonds) in Step trials (gray tick marks). Additionally, the neuron shown in Fig. 5*D* also encodes an SRT-related signal, as indicated by the sudden increase in its activity following the onset of saccades with relatively short SRTs, i.e., in most of the Gap trials and approximately top half of all trials shown in the top panel (Fig. 5*D*). The neuron shown in Fig. 5*E* has a phasic response to the target and another phasic response at ~20 ms after saccadic onset, likely aligned with saccadic offset. By contrast, the neuron shown in Fig. 5*F* had only a phasic response to the target and no saccade-related activity. Thus, rather than being dedicated to visual signal detection, all but the last example neuron was likely involved in visuomotor processing.

We examined whether the target neurons were concentrated more in the lateral half of the arrays, which was more likely to be in the LIP according to the atlas, and again found no evidence for this. We first plotted the 2D distributions of the target neurons as a percentage of recorded neurons from each channel in each of the subjects (Fig. 6), along the anterior-posterior (*x*-axis) and medial-lateral (*y*-axis) dimensions in the

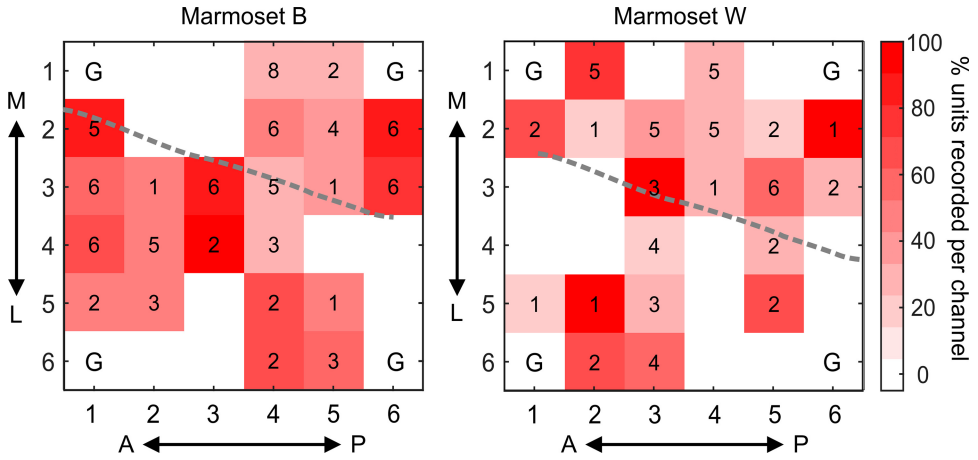

Fig. 6. Topographical distribution of target neurons in both actual number and as a percentage of all neurons recorded from each channel (shown as different shades of red) in *marmosets B* (*left*) and *W* (*right*) in the marmoset posterior parietal cortex. In each plot, the abscissa corresponds to the anterior-posterior axis of the brain, whereas the ordinate corresponds to the medial (*top*)-lateral (*bottom*) axis. The gray dashed lines mark the location of the intraparietal dimple in each animal. M, medial; L, lateral; A, anterior; P, posterior; G, grounding channels.

PPC. We then compared the rate of their detection between halves of the arrays and found no difference in target neuron distribution between the medial and lateral halves (Mann-Whitney *U*-test, $U = 306.5$ and 307, $P = 0.11$ and 0.098, respectively, for *marmosets B* and *W*) or between anterior and posterior halves of all channels ($U = 236$ and 279.5, $P = 0.29$ and 0.56, respectively). It remains possible that an array with more channels and/or covers a greater area of the PPC can detect a better-defined spatial distribution of target neurons.

Correlation between Activity Change and Subsequent SRTs

Now that we found evidence that neurons in the marmoset PPC responded to the gap and the saccadic target, we went on to test for the functional relevance of these responses. We found significant anticorrelations between SRTs and change in neural activities in both the Peristimulus and Visuomotor periods, when the target was contralateral to the recording site. Specifically, we obtained the Peristimulus or Visuomotor responses from all neurons in each trial and calculated their correlation (Spearman's rho) with the subsequent SRTs. If the gap or target neurons were part of the circuitry that plans and generates appropriate saccadic responses, then stronger gap-related or Visuomotor responses should precede efficient responses with shorter SRTs.

As a group, the Peristimulus response of gap neurons showed significant negative correlations with the subsequent SRTs during Gap trials with contralateral targets (1-sample *t*-test against 0 with family-wise error correction: $t_{53} = -3.72$, $P_{adj} = 0.0039$, solid bar, left set, Fig. 7*A*). The same was found for Step trials with contralateral targets ($t_{53} = -2.98$, $P_{adj} = 0.017$, gray filled bar, left set) but not for either trial type with ipsilateral targets ($P_{adj} = 0.44$ and 0.59 respectively, open bars, left set, Fig. 7*A*). Interestingly, the other neurons, the ones without significant Peristimulus response in Gap trials, also showed negative correlation with the SRTs in contralateral Gap trials ($t_{303} = -2.44$, $P_{adj} = 0.041$, solid bar, right set, Fig. 7*A*) but not in other trial types ($P_{adj} \geq 0.59$). We also performed a mixed-model ANOVA to directly compare the correlation coefficients from the two groups of neurons, using task and saccade direction as within-subject variables. We found a main effect of cell type ($F_{1,320} = 8.28$, $P = 0.0043$); gap neurons had overall stronger negative correlation than the other neurons. Thus these findings support the idea that stronger Peristimulus response in gap-sensitive PPC neurons contributes to saccades with shorter SRTs in the Gap task although it could also contribute to a reduction in SRTs in the Step trials. Additionally, this response preparation-related signal was widespread in the PPC and could be detected in neurons that did not respond significantly during the peristimulus period. Intriguingly, such negative correlations were specific to trials with contralateral targets although the Peristimulus responses took place before the target appeared.

For target neurons, we found that their Visuomotor response significantly and negatively correlated with SRTs in contralateral Gap and Step trials (1-sample *t*-test against 0 with family-wise error correction: Gap: $t_{141} = -5.18$, $P_{adj} = 6.1 \times 10^{-6}$, solid bar, Step: $t_{140} = -2.70$, $P_{adj} = 0.031$, shaded bar, left set, Fig. 7*B*). That is, trials with stronger Visuomotor responses

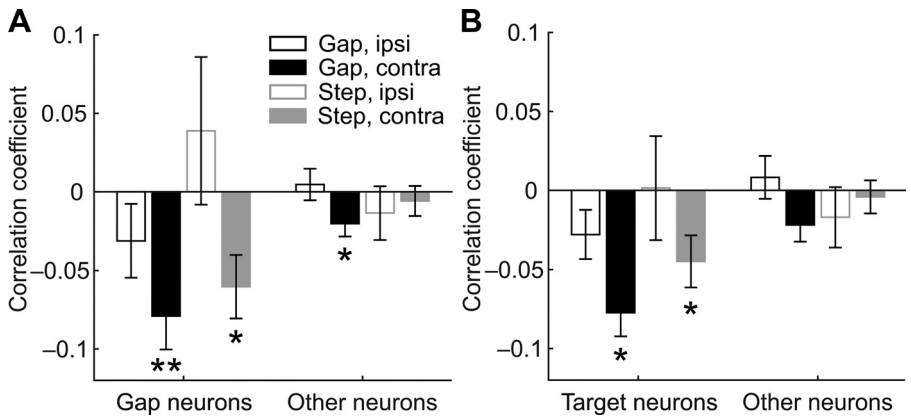

Fig. 7. Correlation coefficients (Spearman's rho) between neuronal response and saccadic reaction times (SRTs). Negative correlations indicate that greater neuronal response preceded shorter SRTs. *A*: correlation coefficients between Peristimulus response of gap neurons (*left*) and the other neurons (*right*) and the SRTs of each type of trials. *B*: correlation coefficients between the Visuomotor response of target neurons (*left*) and the other neurons (*right*) and the SRTs of each type of trials. $^*P < 0.05$, $^{**}P < 0.005$.

from target neurons tended to have a reduction in SRTs. This was not found for neurons that did not respond during the Visuomotor period in either trial types ($P_{adj} \geq 0.11$, right set, Fig. 7*B*). Taken together, the findings demonstrate the presence of a saccade-related signal during both the Peristimulus and Visuomotor periods in the marmoset PPC.

Changes in Gap- or Visual-Related Activity Preceding Short- vs. Long-SRT Saccades

As described above (Fig. 2), we categorized saccades in Gap trials into "short-SRT saccades," defined as those with SRTs in the shortest quartile, and "long-SRT saccades," which included the rest of the trials. Consistent with the anticorrelation found between SRTs and Peristimulus and Visuomotor responses, we found that short-SRT saccades tended to be preceded by stronger neuronal responses especially when the target was contralateral. This effect was observed in both gap and target neurons, as well as in the remainder of the population.

Because neuronal response could be excitatory (i.e., an increase in activity) or inhibitory (i.e., a decrease in activity), we analyzed them separately. Given that the relationship between gap-related response (i.e., Peristimulus response in Gap trials) and SRTs depended on target location (Fig. 7*A*), we also separately analyzed trials involving contralateral vs. ipsilateral saccades. For neurons with excitatory gap-related responses in trials involving contralateral saccades, a two-way ANOVA was performed with cell type (gap vs. other) and saccade type (short vs. long SRT) as the two factors. We found main effects of both saccade type ($F_{1,333} = 26.3$, $P = 4.9 \times 10^{-7}$) and cell type ($F_{1,333} = 11.1$, $P = 0.00095$; Fig. 8*A*, *top*, *left*). A post hoc Tukey's test revealed significantly greater gap-related response preceding short-SRT saccades in both gap neurons ($P = 0.024$, left bars) and other neurons ($P = 7.8 \times 10^{-6}$, right bars, Fig. 8*A*, *top*, *left*). In trials with ipsilateral targets, the same analysis revealed quite a different pattern (Fig. 8*A*, *top*, *right*). We found no effect of cell type ($F_{1,315} = 2.78$, $P = 0.096$) or saccade type ($F_{1,315} = 0.013$, $P = 0.91$). In short, short-SRT saccades to contralateral targets were preceded by greater gap-related activity in PPC neurons.

We then examined the neurons that displayed an inhibitory gap-related response, i.e., decreased in activity level from the fixation to the gap period. Interestingly, the difference between trials with short and long SRT were only found in neurons without significant gap-related or Visuomotor responses. Specifically, in contralateral-saccade trials, we found an effect of cell type ($F_{1,258} = 4.99$, $P = 0.026$) but not of saccade type ($F_{1,258} = 2.78$, $P = 0.097$) or any interaction between the two ($F_{1,258} = 2.32$, $P = 0.13$, Fig. 8*A*, *bottom*, *left*). That is, although the gap neurons did not have a greater reduction in activity before short-SRT saccades (post hoc Tukey's test: $P >$

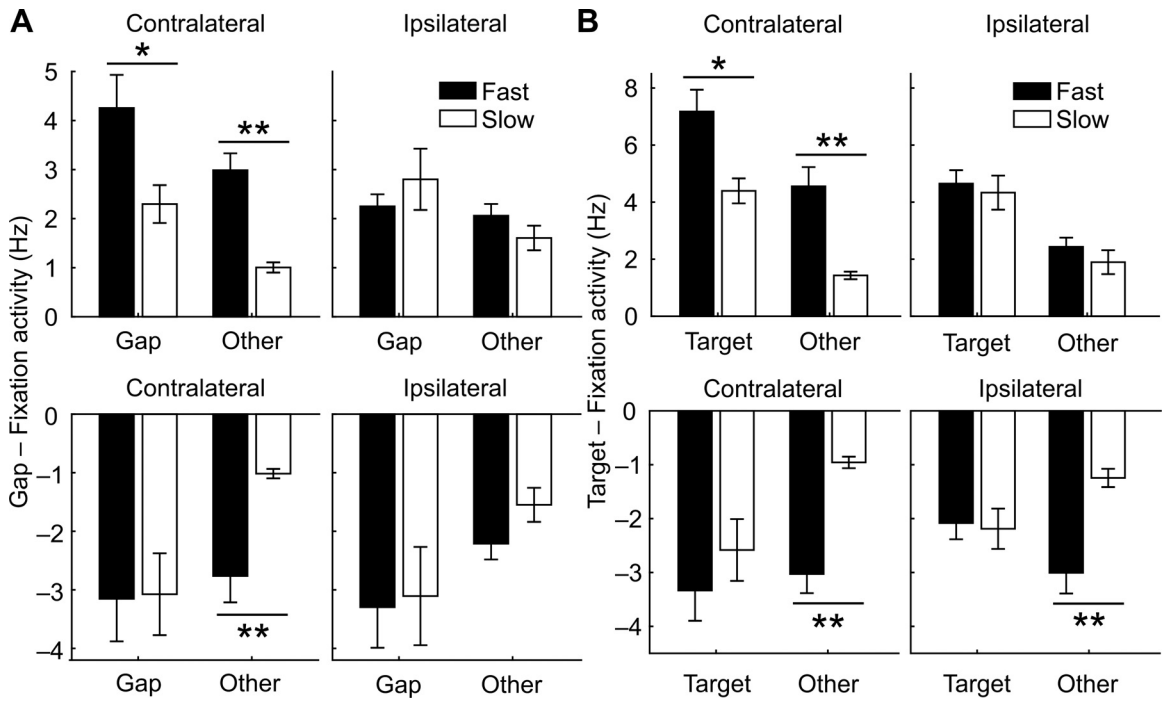

Fig. 8. Neuronal response during the gap and visual periods in Gap trials with short and long saccadic reaction time (SRTs). Short SRTs were defined as those in the shortest quartile of the SRT distribution. *A*: in trials with contralateral targets, gap neurons with an excitatory Peristimulus response did so more strongly in the gap period before short-SRT than long-SRT saccades (left bars, *top*, *left*). The other neurons with a nonsignificant increase in activity also did so more strongly before short-SRT than long-SRT saccades (right bars, *top*, *left*). Gap neurons with an inhibitory response in the Peristimulus period of Gap trials did not respond more strongly before short-SRT saccades (left bars, *bottom*, *left*) although the remaining neurons had a greater reduction in activity before short-SRT saccades (right bars, *bottom*, *left*). In trials with ipsilateral targets, neither type of neurons responded differently before short- and long-SRT saccades (*right*). *B*: in trials with contralateral targets, target neurons with an excitatory response (i.e., those with a significant increase in firing rate in the visual period) responded more strongly in the Visuomotor period before short-SRT than long-SRT saccades (left bars, *top*, *left*). The other neurons with a nonsignificant increase in activity also did so more strongly before short-SRT than long-SRT saccades (right bars, *top*, *left*). Target neurons with an inhibitory response to the gap period did not respond more strongly before short-SRT saccades (left bars, *bottom*, *left*) although the remaining neurons had a greater reduction in activity before short-SRT saccades (right bars, *bottom*, *left*). In trials with ipsilateral targets, although neurons with excitatory responses, significant or not, did not respond differently before short- and long-SRT saccades (*top*, *right*), nontarget neurons showed a greater reduction in Visuomotor activity before short- than long-SRT saccades. $*P < 0.05$, $**P < 0.0005$.

0.99), the other neurons did ($P = 0.00025$). In trials with ipsilateral targets, we did not find any effect of saccade type (main: $F_{1,230} = 0.55$, $P = 0.46$, interaction: $F_{1,230} = 0.17$, $P = 0.68$, Fig. 8*A*, *bottom*, *right*). Taken together, although stronger gap-related responses, significant or not, were more likely followed by short-SRT saccades, this was only the case with contralateral targets.

We then asked whether the relationship between neuronal response and SRT persisted after the onset of the target. Indeed, PPC neurons also tended to have strong target-related, Visuomotor response on trials with short SRTs (Fig. 8*B*). Specifically, on excitatory responses, we found effects of both saccade type ($F_{1,393} = 33.1$, $P = 1.7 \times 10^{-8}$) and cell type ($F_{1,393} = 29.6$, $P = 9.2 \times 10^{-8}$) in contralateral-saccade trials (Fig. 8*B*, *top*, *left*). Both target neurons and other neurons had significantly greater excitatory Visuomotor responses before short-SRT than long-SRT saccades (post hoc Tukey's test, $P = 0.0015$ and 0.00039, respectively). By contrast, among trials with ipsilateral targets, we did not find any effect of saccade type ($F_{1,309} = 0.74$, $P = 0.39$). Among neurons with inhibitory responses, the other neurons had a greater Visuomotor response in contralaterally targeted trials with short SRTs than those with long SRTs (saccade type: $F_{1,209} = 15.4$, $P = 0.00012$, cell type: $F_{1,209} = 7.2$, $P = 0.0079$, post hoc Tukey's test: $P = 1.3 \times 10^{-5}$); the same was not found for target neurons ($P = 0.59$). Similarly in trials with ipsilateral targets, the other neurons but not the target neurons had stronger inhibitory responses around the time of short- compared to long-SRT saccades (saccade type × cell type interaction: $F_{1,246} = 7.08$, $P = 0.0083$; post hoc Tukey's test: target neurons: $P > 0.99$, other neurons: $P = 8.8 \times 10^{-5}$). Taken together, similar to the case of gap-related responses, short-SRT saccades, especially those directed toward contralateral targets, were associated with stronger visual responses in the entire recorded population of PPC neurons.

DISCUSSION

The common marmoset is a promising primate model for human cognition and social interaction. Because saccades provide an essential tool for quantifying complex cognitive processes, it is essential to obtain a detailed understanding of the cortical mechanisms of saccadic control in the marmoset. We therefore recorded single-unit activity using Utah arrays implanted in the PPC of marmosets while they performed visually guided saccades in a gap paradigm and followed up with a microstimulation study upon completion of all recordings (Ghahremani et al. 2019). As previously shown, we found here that marmosets demonstrated a gap effect similar to humans and macaques (Johnston et al. 2018). We found that 15% of all PPC units recorded responded significantly to the gap, and their response magnitude negatively correlated with subsequent SRTs on trials with contralateral targets. The remaining 85% of PPC neurons on average also had a small but significant negative correlation with SRTs on contralateral trials. Additionally, we found 39% of PPC units that responded to the peripheral target, and greater responses in them also correlated with shorter SRTs on contralateral Gap and Step trials. Both types of neurons showed stronger response before short-SRT than long-SRT saccades. Importantly, in the population of PPC neurons recorded, both the gap-related and target-related visuomotor responses were stronger before short-SRT than long-SRT saccades to contralateral targets, which strongly supports a role of the marmoset PPC in modulating saccadic preparation.

Compared to previous studies in other species, the gap-induced reduction in SRT appeared smaller in the marmoset. In macaques, the mean SRT of Step trials and 200-ms Gap trials (regular and express saccades combined) can differ by 100 ms (220 vs. 120 ms; Fischer and Boch 1983). In humans, this difference is much smaller at an average of ~40 ms (180 vs. 140 ms; Saslow 1967). In this study, *marmoset W* had a 31-ms difference in mean SRT (186 vs. 155 ms), which is within the range of variability in human studies (25-70 ms; Wenban-Smith and Findlay 1991). Given *marmoset B*'s very short mean SRT (121 ms) in Step trials, the small difference was likely due to a floor effect. Our animals' relatively short SRTs indicated a sufficient level of training. Although there may be species difference between the nonhuman primates, the marmoset is perhaps more similar to humans in the magnitude of the gap effect.

The Marmoset PPC Contains an Area Homologous to the Macaque LIP

Existing literature and the present study together suggest that the PPC contains an area involved in modulation of saccades across primate species. In human patients with posterior parietal lesions, although the deficits in spatial attention may be the most striking, their impairment in saccadic performance is no less severe (Ptak and Müri 2013). These patients have markedly increased latencies especially for contralateral saccades (Braun et al. 1992; Pierrot-Deseilligny et al. 1991) and significant reduction in express saccades in a gap paradigm (Braun et al. 1992). Our finding of gap-responsive neurons in the PPC was consistent with a role of the area in oculomotor functions in the marmoset, similar to that of the LIP in macaques and parietal eye field in humans.

Although much remains to be learned about the marmoset PPC, it is worthwhile to briefly discuss the present evidence concerning its homology to the macaque PPC from three perspectives, cytoarchitecture, connectivity, and neural response properties (Kaas 1987; Krubitzer 1995). According to the marmoset brain atlas (Paxinos et al. 2012), our arrays, measuring 2.4 × 2.4 mm, should have resided within the anterior and posterior borders of the LIP, which extends 3.5–4 mm rostro-caudally (Paxinos et al. 2012). Mediolaterally, because the arrays straddled the intraparietal dimple, they would have covered part of the atlas-labeled medial intraparietal area (MIP), LIP, and ventral intraparietal area (VIP). The coverage of MIP, which is a reach-related area in macaques, would seem inconsistent with the distribution of saccade-related neurons across the array and with the absence of evoked movements other than saccades and eye blinks (Ghahremani et al. 2019). However, as illustrated in a tracing study (Rosa et al 2009), the putative homolog of LIP is not limited to the lateral side of the dimple in every subject although it remains the most ventral area of the densely myelinated dorsal PPC, which is consistent with the macaque LIP (Blatt et al. 1990). The reason to such variability may be that the dimple is not consistently observed across individuals (Marcello Rosa, personal communication)

and thus does not serve as a reliable landmark for defining subregions in the marmoset PPC.

In addition to cytoarchitecture, functional connectivity and tracing studies have supported the presence of an LIP homolog in the marmoset PPC, given its connections with the FEF and the SC (Ghahremani et al. 2017; Majka et al. 2016; Reser et al. 2013). Similarly in macaque monkeys, the LIP stands out as the only posterior parietal region that projects directly to the SC (Andersen et al. 1990; Lynch et al. 1985). Regarding the frontal connectivity of PPC, all of LIP, VIP, and MIP have reciprocal projections with the FEF in both macaque monkeys (Bakola et al. 2017; Stanton et al. 1995, 2005) and in marmosets (Majka et al. 2016; Reser et al. 2013). Thus the existence of an area homologous to the macaque LIP in the marmoset PPC is supported by studies of connectivity, but its precise boundary remains unclear.

The present study is one of the first to provide evidence concerning the third criterion for homology, neural response properties (Kaas 1987; Krubitzer 1995). In macaque monkeys, distinct from the LIP, the MIP is specialized for reaches (Gnadt and Andersen 1988; Snyder et al. 1997), and lesions of this area do not affect contralateral saccade choices (Christopoulos et al. 2015). If the marmoset MIP were located on the medial bank of the intraparietal dimple, gap-sensitive neurons should be detected less frequently on the medial side of the array, which was not the case. In the macaque PPC, it is now clear that oculomotor and visuomanual signals are mixed within areas either primarily involved in eye (Dickinson et al. 2003) or arm movements (Archambault et al. 2009; Battaglia-Mayer et al. 2001). Although the evidence suggests cross-modal integration and gradual transitions from one functional domain to another in the macaque PPC (Hadjidimitrakis et al. 2019), in the marmoset PPC, no such gradual change in neuronal activity or evoked response (Ghahremani et al. 2019) was observed. Taken together, the three lines of evidence support the existence of a marmoset homolog of the macaque LIP in the PPC and suggest that this homolog may be located differently with reference to the intraparietal dimple.

Marmoset PPC Neurons Can Modulate Saccadic Preparation and Execution

The specific oculomotor function played by the primate PPC remains a topic of active investigation. Rather than being directly involved in saccade planning, the PPC likely contributes to the modulation of saccades through its role in attention and perception (Bisley and Goldberg 2003). Previous studies have identified visual neurons (Andersen et al. 1985), e.g., those responding to the onset (Gottlieb et al. 1998; Kubanek et al. 2013) or offset (Ben Hamed and Duhamel 2002) of salient or relevant targets, as well as neurons responsive to both visual target and saccadic onset (Colby et al. 1996; Gottlieb et al. 2005), with differential distribution along the dorsal-ventral extent of the macaque LIP (Chen et al. 2016). Similarly, in the marmoset PPC, we observed neurons responsive to fixation offset and those responsive to target onset and saccadic onset. We speculate that the gap-period activities in the PPC can directly enhance the pretarget activities observed in SC saccade neurons in macaques (Dorris et al. 1997) or weaken the activity in SC fixation neurons via reduced excitatory input (Sommer and Wurtz 2000), and those responsive to the target can provide additional input that drives SC neurons over the saccade threshold.

Although the percentage of gap-sensitive neurons found here may appear less than in macaque LIP (Chen et al. 2013), it should be noted that we included all single units detected in our chronic arrays without imposing any criterion other than a firing rate greater than 0.3 Hz. The earliest gap-related response in gap neurons started at around 70 ms after fixation offset, which is comparable to the earliest response in macaque FEF (Tinsley and Everling 2002) and LIP (Ben Hamed and Duhamel 2002; Chen et al. 2013). The magnitude of response in some of our gap neurons (e.g., Fig. 3*E*) is comparable to the strongest gap-responding neuron in some macaque monkeys (Chen et al. 2013). Notably, even neurons without a significant gap-related response still responded more strongly during the gap period before short- than long-SRT saccades to contralateral targets. Additionally, the gap-related response of the entire recorded neuronal population negatively correlated with the subsequent SRTs on Gap trials with contralateral targets, although the correlations were stronger in gap-sensitive neurons. Such correlation has been observed in macaque monkeys in the LIP (Chen et al. 2013), the SC (Dorris et al. 1997; Dorris and Munoz 1998; Everling et al. 1999), and the FEF (Everling and Munoz 2000), which suggests a concerted preparatory process at the circuit level. Our finding indicates that this circuitry and process are shared across the two species, a hypothesis that will need to be tested by single-unit recordings from other oculomotor areas in the marmoset.

It should be noted that the gap-period activity of PPC neurons only negatively correlated with the SRTs when the targets were contralateral although their gap-related response was independent of the target location. These neurons also went on to show a second response that was stronger following the onset of contralateral targets. Both observations suggest that their gap-related response only contributed to the preparation for saccades to contralateral targets, likely via the ipsilateral PPC-SC pathway, which controls saccades contralaterally. This directionality also existed for the difference between short- and long-SRT saccades. Together, these findings support a role of the PPC in advanced motor preparation for the gap effect and express-like saccades (Chen et al. 2013, 2016; Munoz and Fecteau 2002).

In target neurons, we also found that their target-related activity was correlated with subsequent SRTs, and their target-related activity was stronger before short- than long-SRT saccades. Thus the target neurons were likely not equivalent to LIP visual neurons in macaques, which had a spatially tuned response to the target in memory-guided saccade tasks and did not show activities correlated with the SRTs in the gap task (Chen et al. 2013). Because our marmosets did not perform memory-guided saccades on the same sessions analyzed here, we were unable to isolate the purely visual neurons that may exist in the marmoset PPC. Also, without receptive-field mapping, a neuron had to be sensitive to one of the two locations to be considered a target neuron. Hence, both the percentage of target neurons and the magnitude of the target-related response were likely underestimated. Much of the target neuron activity was more complex than a purely visual response. As shown in RESULTS, two-thirds of the gap neurons were also target neurons, constituting the 25% of target neurons that also showed a stronger target-related response in Gap trials. Additionally, the

activity of target neurons showed a strong effect of target location/saccade direction; some also had an additional response aligned to saccadic onset or offset. Given the 100-ms interval used in the definition of the target neurons, these neurons may also be involved in modulating the preparatory signal in the oculomotor circuitry and contribute to the gap effect in general via projections to the SC.

Overall, similar to studies using macaque monkeys (e.g., Everling et al. 1998; Sommer and Wurtz 2000; Tinsley and Everling 2002), we found gap- and target-responsive neurons under the same definition. Without a delayed-saccade task, we were unable to differentiate purely visual from visuomotor neurons although both types are likely present in the marmoset PPC, as suggested by our examples. The strength of the gap-related response in gap neurons was comparable to that in some of the macaque monkeys in previous studies (Chen et al. 2013). Because the receptive field of target neurons were not mapped, it was expected that the magnitude of their target-related response was smaller in our study (Chen et al. 2013). For the same reason, the actual abundance of visual and visuomotor neurons is likely higher than described here.

Conclusion

In summary, we conducted the first single-unit recording study in the marmoset PPC and observed both peristimulus and target-related activities, which were correlated with the SRTs especially on contralateral Gap trials. The neuronal population including all units detected responded more strongly during the gap period preceding short- than long-SRT saccades, consistent with the critical role of the PPC in express saccades in humans (Braun et al. 1992). Together with our recent study on evoked saccades through the same PPC arrays (Ghahremani et al. 2019), our findings support the hypothesis that the marmoset PPC contains an area homologous to the macaque LIP. We suggest that the common marmoset is a highly valuable model for understanding the circuit-level dynamics underlying oculomotor processes and the pathological changes that produce the well-documented oculomotor deficits observed in neuropsychiatric disorders.

ACKNOWLEDGMENTS

We thank N. Hague, C. Vander Tuin, W. Froese, and K. Faubert for surgical assistance and care of the experimental animals.

GRANTS

This research was supported by a Foundation grant from the Canadian Institutes of Health Research (FRN 148365) to S. Everling and postdoctoral fellowships from the Canadian Institutes of Health Research and the BrainsCAN Initiative to L. Ma.

DISCLOSURES

No conflicts of interest, financial or otherwise, are declared by the authors.

AUTHOR CONTRIBUTIONS

L.M., L.K.H., K.D.J., and S.E. performed experiments; L.M. and J.S. analyzed data; L.M. interpreted results of experiments; L.M. and M.G. prepared figures; L.M. drafted manuscript; L.M., J.S., M.G., L.K.H., K.D.J., and S.E. edited and revised manuscript; K.D.J. and S.E. conceived and designed research; S.E. approved final version of manuscript.

REFERENCES

Andersen RA, Asanuma C, Cowan WM. Callosal and prefrontal associational projecting cell populations in area 7A of the macaque monkey: a study using retrogradely transported fluorescent dyes. *J Comp Neurol* 232: 443–455, 1985. doi:10.1002/cne.902320403.

Andersen RA, Bracewell RM, Barash S, Gnadt JW, Fogassi L. Eye position effects on visual, memory, and saccade-related activity in areas LIP and 7a of macaque. J Neurosci 10: 1176–1196, 1990.

Archambault PS, Caminiti R, Battaglia-Mayer A. Cortical mechanisms for online control of hand movement trajectory: the role of the posterior parietal cortex. *Cereb Cortex* 19: 2848–2864, 2009. doi:10.1093/cercor/bhp058.

Bakola S, Passarelli L, Huynh T, Impieri D, Worthy KH, Fattori P, Galletti C, Burman KJ, Rosa MGP. Cortical afferents and myeloarchitecture distinguish the medial intraparietal area (MIP) from neighboring subdivisions of the macaque cortex. *eNeuro* 4: ENEURO.0344–17.2017, 2017.

Battaglia-Mayer A, Ferraina S, Genovesio A, Marconi B, Squatrito S, Molinari M, Lacquaniti F, Caminiti R. Eye-hand coordination during reaching. II. An analysis of the relationships between visuomanual signals in parietal cortex and parieto-frontal association projections. *Cereb Cortex* 11: 528–544, 2001. doi:10.1093/cercor/11.6.528.

Ben Hamed S, Duhamel JR. Ocular fixation and visual activity in the monkey lateral intraparietal area. *Exp Brain Res* 142: 512–528, 2002. doi:10.1007/s00221-001-0954-z.

Ben Hamed S, Duhamel J-R, Bremmer F, Graf W. Representation of the visual field in the lateral intraparietal area of macaque monkeys: a quantitative receptive field analysis. *Exp Brain Res* 140: 127–144, 2001. doi:10.1007/s002210100785.

Benjamini Y, Hochberg Y. Controlling the false discovery rate: a practical and powerful approach to multiple testing. *J R Stat Soc B* 57: 289–300, 1995. doi:10.1111/j.2517-6161.1995.tb02031.x.

Bisley JW, Goldberg ME. Neuronal activity in the lateral intraparietal area and spatial attention. *Science* 299: 81–86, 2003. doi:10.1126/science.1077395.

Blatt GJ, Andersen RA, Stoner GR. Visual receptive field organization and cortico-cortical connections of the lateral intraparietal area (area LIP) in the macaque. *J Comp Neurol* 299: 421–445, 1990. doi:10.1002/cne.902990404.

Braun D, Weber H, Mergner T, Schulte-Mönting J. Saccadic reaction times in patients with frontal and parietal lesions. *Brain* 115: 1359–1386, 1992. doi:10.1093/brain/115.5.1359.

Brown MRG, DeSouza JFX, Goltz HC, Ford K, Menon RS, Goodale MA, Everling S. Comparison of memory- and visually guided saccades using event-related fMRI. *J Neurophysiol* 91: 873–889, 2004. doi:10.1152/jn.00382.2003.

Chen M, Liu Y, Wei L, Zhang M. Parietal cortical neuronal activity is selective for express saccades. *J Neurosci* 33: 814–823, 2013. doi:10.1523/JNEUROSCI.2675-12.2013.

Chen M, Li B, Guang J, Wei L, Wu S, Liu Y, Zhang M. Two subdivisions of macaque LIP process visual-oculomotor information differently. *Proc Natl Acad Sci USA* 113: E6263–E6270, 2016. doi:10.1073/pnas.1605879113.

Christopoulos VN, Bonaiuto J, Kagan I, Andersen RA. Inactivation of parietal reach region affects reaching but not saccade choices in internally guided decisions. *J Neurosci* 35: 11719–11728, 2015. doi:10.1523/JNEUROSCI.1068-15.2015.

Colby CL, Duhamel JR, Goldberg ME. Visual, presaccadic, and cognitive activation of single neurons in monkey lateral intraparietal area. *J Neurophysiol* 76: 2841–2852, 1996. doi:10.1152/jn.1996.76.5.2841.

Collins CE, Lyon DC, Kaas JH. Distribution across cortical areas of neurons projecting to the superior colliculus in new world monkeys. *Anat Rec A Discov Mol Cell Evol Biol* 285: 619–627, 2005. doi:10.1002/ar.a.20207.

DeSouza JFX, Menon RS, Everling S. Preparatory set associated with pro-saccades and anti-saccades in humans investigated with event-related FMRI. *J Neurophysiol* 89: 1016–1023, 2003. doi:10.1152/jn.00562.2002.

Dias EC, Bruce CJ. Physiological correlate of fixation disengagement in the primate's frontal eye field. *J Neurophysiol* 72: 2532–2537, 1994. doi:10.1152/jn.1994.72.5.2532.

Dickey AS, Suminski A, Amit Y, Hatsopoulos NG. Single-unit stability using chronically implanted multielectrode arrays. *J Neurophysiol* 102: 1331–1339, 2009. doi:10.1152/jn.90920.2008.

Dickinson AR, Calton JL, Snyder LH. Nonspatial saccade-specific activation in area LIP of monkey parietal cortex. *J Neurophysiol* 90: 2460–2464, 2003. doi:10.1152/jn.00788.2002.

Dorris MC, Munoz DP. A neural correlate for the gap effect on saccadic reaction times in monkey. *J Neurophysiol* 73: 2558–2562, 1995. doi:10.1152/jn.1995.73.6.2558.

Dorris MC, Munoz DP. Saccadic probability influences motor preparation signals and time to saccadic initiation. *J Neurosci* 18: 7015–7026, 1998. doi:10.1523/JNEUROSCI.18-17-07015.1998.

Dorris MC, Paré M, Munoz DP. Neuronal activity in monkey superior colliculus related to the initiation of saccadic eye movements. *J Neurosci* 17: 8566–8579, 1997. doi:10.1523/JNEUROSCI.17-21-08566.1997.

Everling S, Munoz DP. Neuronal correlates for preparatory set associated with pro-saccades and anti-saccades in the primate frontal eye field. *J Neurosci* 20: 387–400, 2000. doi:10.1523/JNEUROSCI.20-01-00387.2000.

Everling S, Krappmann P, Preuss S, Brand A, Flohr H. Hypometric primary saccades of schizophrenics in a delayed-response task. *Exp Brain Res* 111: 289–295, 1996. doi:10.1007/BF00227306.

Everling S, Paré M, Dorris MC, Munoz DP. Comparison of the discharge characteristics of brain stem omnipause neurons and superior colliculus fixation neurons in monkey: implications for control of fixation and saccade behavior. *J Neurophysiol* 79: 511–528, 1998. doi:10.1152/jn.1998.79.2.511.

Everling S, Dorris MC, Klein RM, Munoz DP. Role of primate superior colliculus in preparation and execution of anti-saccades and pro-saccades. *J Neurosci* 19: 2740–2754, 1999. doi:10.1523/JNEUROSCI.19-07-02740.1999.

Fendrich R, Hughes HC, Reuter-Lorenz PA. Fixation-point offsets reduce the latency of saccades to acoustic targets. *Percept Psychophys* 50: 383–387, 1991. doi:10.3758/BF03212231.

Fischer B, Boch R. Saccadic eye movements after extremely short reaction times in the monkey. *Brain Res* 260: 21–26, 1983. doi:10.1016/0006-8993(83)90760-6.

Gaymard B, Rivaud S, Cassarini JF, Dubard T, Rancurel G, Agid Y, Pierrot-Deseilligny C. Effects of anterior cingulate cortex lesions on ocular saccades in humans. *Exp Brain Res* 120: 173–183, 1998. doi:10.1007/s002210050391.

Ghahremani M, Hutchison RM, Menon RS, Everling S. Frontoparietal functional connectivity in the common marmoset. *Cereb Cortex* 27: 3890–3905, 2017. doi:10.1093/cercor/bhw198.

Ghahremani M, Johnston KD, Ma L, Hayrynen LK, Everling S. Electrical microstimulation evokes saccades in posterior parietal cortex of common marmosets. *J Neurophysiol* 122: 1765–1776, 2019. doi:10.1152/jn.00417.2019.

Gnadt JW, Andersen RA. Memory related motor planning activity in posterior parietal cortex of macaque. *Exp Brain Res* 70: 216–220, 1988.

Gooding DC, Basso MA. The tell-tale tasks: a review of saccadic research in psychiatric patient populations. *Brain Cogn* 68: 371–390, 2008. doi:10.1016/j.bandc.2008.08.024.

Gottlieb JP, Kusunoki M, Goldberg ME. The representation of visual salience in monkey parietal cortex. *Nature* 391: 481–484, 1998. doi:10.1038/35135.

Gottlieb J, Kusunoki M, Goldberg ME. Simultaneous representation of saccade targets and visual onsets in monkey lateral intraparietal area. *Cereb Cortex* 15: 1198–1206, 2005. doi:10.1093/cercor/bhi002.

Groppe DM, Urbach TP, Kutas M. Mass univariate analysis of event-related brain potentials/fields I: a critical tutorial review. *Psychophysiology* 48: 1711–1725, 2011. doi:10.1111/j.1469-8986.2011.01273.x.

Hadjidimitrakis K, Bakola S, Wong YT, Hagan MA. Mixed spatial and movement representations in the primate posterior parietal cortex. *Front Neural Circuits* 13: 15, 2019. doi:10.3389/fncir.2019.00015.

Hanes DP, Schall JD. Neural control of voluntary movement initiation. *Science* 274: 427–430, 1996. doi:10.1126/science.274.5286.427.

Harris KD, Thiele A. Cortical state and attention. *Nat Rev Neurosci* 12: 509–523, 2011. doi:10.1038/nrn3084.

Hutton SB. Cognitive control of saccadic eye movements. *Brain Cogn* 68: 327–340, 2008. doi:10.1016/j.bandc.2008.08.021.

Hutton SB, Ettinger U. The antisaccade task as a research tool in psychopathology: a critical review. *Psychophysiology* 43: 302–313, 2006. doi:10.1111/j.1469-8986.2006.00403.x.

Johnston KD, Barker K, Schaeffer L, Schaeffer D, Everling S. Methods for chair restraint and training of the common marmoset on oculomotor tasks. *J Neurophysiol* 119: 1636–1646, 2018. doi:10.1152/jn.00866.2017.

Kaas JH. The organization of neocortex in mammals: implications for theories of brain function. *Annu Rev Psychol* 38: 129–151, 1987. doi:10.1146/annurev.ps.38.020187.001021.

Keller EL, Edelman JA. Use of interrupted saccade paradigm to study spatial and temporal dynamics of saccadic burst cells in superior colliculus in monkey. *J Neurophysiol* 72: 2754–2770, 1994.

Klein C, Heinks T, Andresen B, Berg P, Moritz S. Impaired modulation of the saccadic contingent negative variation preceding antisaccades in schizophrenia. *Biol Psychiatry* 47: 978–990, 2000. doi:10.1016/S0006-3223(00)00234-1.

Krubitzer L. The organization of neocortex in mammals: are species differences really so different? *Trends Neurosci* 18: 408–417, 1995. doi:10.1016/0166-2236(95)93938-T.

Kubanek J, Wang C, Snyder LH. Neuronal responses to target onset in oculomotor and somatomotor parietal circuits differ markedly in a choice task. *J Neurophysiol* 110: 2247–2256, 2013. doi:10.1152/jn.00968.2012.

Kurylo DD, Skavenski AA. Eye movements elicited by electrical stimulation of area PG in the monkey. *J Neurophysiol* 65: 1243–1253, 1991. doi:10.1152/jn.1991.65.6.1243.

Liu C, Ye FQ, Yen CCC, Newman JD, Glen D, Leopold DA, Silva AC. A digital 3D atlas of the marmoset brain based on multi-modal MRI. *Neuroimage* 169: 106–116, 2018. doi:10.1016/j.neuroimage.2017.12.004.

Lynch JC, Graybiel AM, Lobeck LJ. The differential projection of two cytoarchitectonic subregions of the inferior parietal lobule of macaque upon the deep layers of the superior colliculus. *J Comp Neurol* 235: 241–254, 1985.

Majka P, Chaplin TA, Yu H-H, Tolpygo A, Mitra PP, Wójcik DK, Rosa MG. Towards a comprehensive atlas of cortical connections in a primate brain: Mapping tracer injection studies of the common marmoset into a reference digital template. *J Comp Neurol* 524: 2161–2181, 2016. doi:10.1002/cne.24023.

Miller CT, Freiwald WA, Leopold DA, Mitchell JF, Silva AC, Wang X. Marmosets: a neuroscientific model of human social behavior. *Neuron* 90: 219–233, 2016. doi:10.1016/j.neuron.2016.03.018.

Mitchell JF, Reynolds JH, Miller CT. Active vision in marmosets: a model system for visual neuroscience. *J Neurosci* 34: 1183–1194, 2014. doi:10.1523/JNEUROSCI.3899-13.2014.

Mitchell JF, Priebe NJ, Miller CT. Motion dependence of smooth pursuit eye movements in the marmoset. *J Neurophysiol* 113: 3954–3960, 2015. doi:10.1152/jn.00197.2015.

Munoz DP, Everling S. Look away: the anti-saccade task and the voluntary control of eye movement. *Nat Rev Neurosci* 5: 218–228, 2004. doi:10.1038/nrn1345.

Munoz DP, Fecteau JH. Vying for dominance: dynamic interactions control visual fixation and saccadic initiation in the superior colliculus. *Prog Brain Res* 140: 3–19, 2002. doi:10.1016/S0079-6123(02)40039-8.

Nicolelis MAL, Dimitrov D, Carmena JM, Crist R, Lehew G, Kralik JD, Wise SP. Chronic, multisite, multielectrode recordings in macaque monkeys. *Proc Natl Acad Sci USA* 100: 11041–11046, 2003. doi:10.1073/pnas.1934665100.

Paré M, Munoz DP. Saccadic reaction time in the monkey: advanced oculomotor programs is primarily responsible for occurrence preparation of express saccade occurrence. *J Neurophysiol* 76: 3666–3681, 1996. doi:10.1152/jn.1996.76.6.3666.

Paxinos G, Watson C, Petrides M, Rosa M, Tokuno H. *The Marmoset Brain in Stereotaxic Coordinates*. London: Elsevier, 2012.

Pierrot-Deseilligny C, Rosa A, Masmoudi K, Rivaud S, Gaymard B. Saccade deficits after a unilateral lesion affecting the superior colliculus. *J Neurol Neurosurg Psychiatry* 54: 1106–1109, 1991. doi:10.1136/jnnp.54.12.1106.

Ptak R, Müri RM. The parietal cortex and saccade planning: lessons from human lesion studies. *Front Hum Neurosci* 7: 254, 2013. doi:10.3389/fnhum.2013.00254.

Reimer J, Froudarakis E, Cadwell CR, Yatsenko D, Denfield GH, Tolias AS. Pupil fluctuations track fast switching of cortical states during quiet wakefulness. *Neuron* 84: 355–362, 2014. doi:10.1016/j.neuron.2014.09.033.

Reser DH, Burman KJ, Yu H-H, Chaplin TA, Richardson KE, Worthy KH, Rosa MGP. Contrasting patterns of cortical input to architectural subdivisions of the area 8 complex: a retrograde tracing study in marmoset monkeys. *Cereb Cortex* 23: 1901–1922, 2013. doi:10.1093/cercor/bhs177.

Reuter-Lorenz PA, Hughes HC, Fendrich R. The reduction of saccadic latency by prior offset of the fixation point: an analysis of the gap effect. *Percept Psychophys* 49: 167–175, 1991. doi:10.3758/BF03205036.

Richmond BJ, Optican LM. Temporal encoding of two-dimensional patterns by single units in primate inferior temporal cortex. II. Quantification of response waveform. *J Neurophysiol* 57: 147–161, 1987. doi:10.1152/jn.1987.57.1.147.

Rosa MGP, Palmer SM, Gamberini M, Burman KJ, Yu H-H, Reser DH, Bourne JA, Tweedale R, Galletti C. Connections of the dorsomedial visual area: pathways for early integration of dorsal and ventral streams in extrastriate cortex. *J Neurosci* 29: 4548–4563, 2009. doi:10.1523/JNEUROSCI.0529-09.2009.

Saslow MG. Effects of components of displacement-step stimuli upon latency for saccadic eye movement. *J Opt Soc Am* 57: 1024–1029, 1967. doi:10.1364/JOSA.57.001024.

Shibutani H, Sakata H, Hyvärinen J. Saccade and blinking evoked by microstimulation of the posterior parietal association cortex of the monkey. *Exp Brain Res* 55: 1–8, 1984. doi:10.1007/BF00240493.

Snyder LH, Batista AP, Andersen RA. Coding of intention in the posterior parietal cortex. *Nature* 386: 167–170, 1997. doi:10.1038/386167a0.

Sommer MA. Express saccades elicited during visual scan in the monkey. *Vision Res* 34: 2023–2038, 1994. doi:10.1016/0042-6989(94)90030-2.

Sommer MA, Wurtz RH. Composition and topographic organization of signals sent from the frontal eye field to the superior colliculus. *J Neurophysiol* 83: 1979–2001, 2000. doi:10.1152/jn.2000.83.4.1979.

Stanton GB, Bruce CJ, Goldberg ME. Topography of projections to posterior cortical areas from the macaque frontal eye fields. *J Comp Neurol* 353: 291–305, 1995. doi:10.1002/cne.903530210.

Stanton GB, Friedman HR, Dias EC, Bruce CJ. Cortical afferents to the smooth-pursuit region of the macaque monkey's frontal eye field. *Exp Brain Res* 165: 179–192, 2005. doi:10.1007/s00221-005-2292-z.

Thier P, Andersen RA. Electrical microstimulation suggests two different forms of representation of head-centered space in the intraparietal sulcus of rhesus monkeys. *Proc Natl Acad Sci USA* 93: 4962–4967, 1996. doi:10.1073/pnas.93.10.4962.

Thier P, Andersen RA. Electrical microstimulation distinguishes distinct saccade-related areas in the posterior parietal cortex. *J Neurophysiol* 80: 1713–1735, 1998. doi:10.1152/jn.1998.80.4.1713.

Thompson KG, Hanes DP, Bichot NP, Schall JD. Perceptual and motor processing stages identified in the activity of macaque frontal eye field neurons during visual search. *J Neurophysiol* 76: 4040–4055, 1996. doi:10.1152/jn.1996.76.6.4040.

Tinsley CJ, Everling S. Contribution of the primate prefrontal cortex to the gap effect. *Prog Brain Res* 140: 61–72, 2002. doi:10.1016/S0079-6123(02)40042-8.

Van Essen DC, Drury HA, Dickson J, Harwell J, Hanlon D, Anderson CH. An integrated software suite for surface-based analyses of cerebral cortex. *J Am Med Inform Assoc* 8: 443–459, 2001. doi:10.1136/jamia.2001.0080443.

Vinck M, Batista-Brito R, Knoblich U, Cardin JA. Arousal and locomotion make distinct contributions to cortical activity patterns and visual encoding. *Neuron* 86: 740–754, 2015. doi:10.1016/j.neuron.2015.03.028.

Waitzman DM, Ma TP, Optican LM, Wurtz RH. Superior colliculus neurons mediate the dynamic characteristics of saccades. *J Neurophysiol* 66: 1716–1737, 1991. doi:10.1152/jn.1991.66.5.1716.

Wenban-Smith MG, Findlay JM. Express saccades: is there a separate population in humans? *Exp Brain Res* 87: 218–222, 1991. doi:10.1007/BF00228523.

Zavitz E, Yu HH, Rowe EG, Rosa MGP, Price NSC. Rapid adaptation induces persistent biases in population codes for visual motion. *J Neurosci* 36: 4579–4590, 2016. doi:10.1523/JNEUROSCI.4563-15.2016.